

Optical phase estimation via the coherent state and displaced-photon counting

Shuro Izumi,^{1,2} Masahiro Takeoka,¹ Kentaro Wakui,¹ Mikio Fujiwara,¹ Kazuhiro Ema,² and Masahide Sasaki¹

¹*National Institute of Information and Communications Technology, 4-2-1 Nukui-kita, Koganei, Tokyo 184-8795, Japan*

²*Sophia University, 7-1 Kioicho, Chiyoda-ku, Tokyo 102-8554, Japan*

(Received 17 April 2016; published 22 September 2016)

We consider the phase sensing via a weak optical coherent state at quantum limit precision. A detection scheme for the phase estimation is proposed, which is inspired by the suboptimal quantum measurement in coherent optical communication. We theoretically analyze a performance of our detection scheme, which we call the displaced-photon counting, for phase sensing in terms of the Fisher information and show that the displaced-photon counting outperforms the static homodyne and heterodyne detections in a wide range of the target phase. The proof-of-principle experiment is performed with linear optics and a superconducting nanowire single-photon detector. The result shows that our scheme overcomes the limit of the ideal homodyne measurement, even under practical imperfections.

DOI: [10.1103/PhysRevA.94.033842](https://doi.org/10.1103/PhysRevA.94.033842)

I. INTRODUCTION

Quantum optical sensing has attracted both fundamental and practical interest (see, for example, [1] and references therein). In particular, sensing of the unknown phase ϕ of the optical signal state is a simple but practically important problem. A typical setup of the optical phase estimation consists of a probe state, unitary (unknown) phase shifting, and the detection (and estimation) step (Fig. 1). The precision of estimation is usually evaluated by a mean-square error $\text{Var}[\hat{\phi}] = E[(\hat{\phi} - E[\hat{\phi}])^2]$ of the estimator $\hat{\phi}$. For an unbiased estimator, it is well known that its ultimate lower bound is given by the quantum Cramer-Rao bound:

$$\text{Var}[\hat{\phi}] \geq \frac{1}{MH(\phi)}, \quad (1)$$

where M is the number of data and $H(\phi)$ is the quantum Fisher information (QFI) [2] which is a function of state $\rho(\phi)$.

Two questions are particularly interesting and have attracted attention so far: (1) what probe state maximizes $H(\phi)$ and (2) how to saturate the bound in a realistic experimental setting. For the first question, it has been shown that highly nonclassical states, such as squeezed states [3–5] or NOON states [6–9], could beat the QFI of the coherent state, which is often called the “standard quantum limit” scaling as $1/N$, where N is the average photon number of the state. Moreover, ideally it reaches the so-called Heisenberg limit scaling $1/N^2$. However, it has been also revealed that these nonclassical states are very fragile to losses (unless using extremely nontrivial states) [10], which is an unavoidable imperfection in real experimentation. In this sense, for some practical applications in which one has to admit high losses, the coherent state is still a useful option for phase sensing since the coherent state preserves its coherence and purity even under high losses. In the following, we concentrate on phase estimation by coherent-state probes.

The second question is related to the choice of the detection strategy. For a given system (i.e., given probe state and measurement), the lower bound of $\text{Var}[\hat{\phi}]$ is determined by the classical Fisher information (FI) $F(\phi)$ and the QFI for a given probe state is defined as the maximum $F(\phi)$ over all possible quantum measurement [2]. Thus, by definition, the

following inequality holds for any given states:

$$H(\phi) \geq F(\phi). \quad (2)$$

The question is to find the optimal measurement that saturates this inequality, preferably for any ϕ . For a coherent state, it is known that homodyne measurement can saturate (2) around a certain ϕ [11]. This is a nice consequence but not always practical, since the FI decrease quickly if ϕ is far from the specific point. Though globally optimal measurement is possible by adaptive homodyne detection with a real-time feedback system [12], it may not be implementable for some applications, especially when the number of data is highly limited. In addition, a finite bandwidth of the adaptive feedback operation causes some restrictions on the system parameters, such as the repetition rate of source and detector. Therefore it is still worth investigating the static measurement which could surpass the FI of the homodyne measurement in a wide range of ϕ .

In this paper, we propose and experimentally demonstrate a simple detection strategy for the coherent-state phase estimation. Our detection scheme is inspired by the recent progress of “quantum receiver” technology developed in the field of quantum optical communication. In optical communication at the very low power regime, it is known that homodyne or heterodyne measurements are not optimal to minimize the error of discriminating modulated coherent-state signals [13]. In the last decade, a practical quantum receiver configuration superior to homodyne and heterodyne receivers has been proposed for various sets of signals [14–21] and is successfully demonstrated with the current technology [22–29]. Our basic idea is to apply these receivers—originally designed for state discrimination—for a different purpose, i.e., the phase estimation. Specifically, we employ the simplest static receiver technique, which we call the displaced-photon counting [14,18,25,30], consisting of displacement operation and a photon detector (with no adaptive feedback). We show that in a wide range of ϕ , our scheme works better than homodyne and heterodyne receivers in terms of FI. The concept is also demonstrated experimentally.

The paper is organized as follows. In Sec. II, we propose a detection scheme for the coherent-state phase estimation and then analyze its performance in terms of the Fisher information

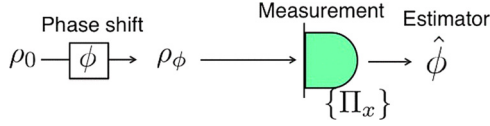


FIG. 1. Schematic of general phase estimation.

formalism. Section III is devoted to the proof-of-principle experiment of the proposed scheme. Section IV concludes the paper.

II. DISPLACED-PHOTON COUNTING FOR PHASE ESTIMATION

In this section, after a brief reminder of the Fisher information formalism, we propose a simple detection scheme for phase estimation which we call the displaced-photon counting. We theoretically investigate its performance in terms of the FI and then compare it with that for other existing technologies, such as homodyne and heterodyne detections.

As mentioned in the Introduction, the QFI sets the minimum bound of the variance for a given state. For pure states, the QFI is simply given by [11]

$$H = 4\Delta K^2, \quad (3)$$

where $\Delta K^2 = \langle K^2 \rangle - \langle K \rangle^2$ is the fluctuation of the photon number of the state and $K = a^\dagger a$ is the photon number operator. ΔK^2 is invariant with respect to the phase shift ϕ , and thus the QFI is simply determined by the initial state ρ_0 . Equation (3) allows us to explicitly calculate the QFI for the coherent state, which simply turns out to be $H_{\text{coh}} = 4\alpha^2$.

The performance of a given system, including both the state and the measurement, can be theoretically analyzed by the FI [31]. The FI is defined as

$$F(\phi) = \int \frac{1}{p(x|\phi)} \left(\frac{\partial p(x|\phi)}{\partial \phi} \right)^2, \quad (4)$$

where $p(x|\phi)$ is a conditional probability of obtaining an outcome x for given phase shift ϕ . This conditional probability is a function of the state ρ_ϕ and the measurement, described by a positive operator valued measure (POVM) $\{\Pi_x\}$ satisfying $\int dx \Pi_x = I$ as

$$p(x|\phi) = \text{Tr}[\Pi_x \rho_\phi]. \quad (5)$$

Note that for discrete measurement observables such as photon numbers, the integration in (4) should be replaced with a sum of all measurement outcomes.

Figure 2 shows a simple schematic of the phase estimation of the coherent state with the displaced-photon counting. The displacement operation $D(\beta)$ is a linear operation shifting the amplitude of the coherent state $|\gamma\rangle$ as $D(\beta)|\gamma\rangle = |\beta + \gamma\rangle$. In

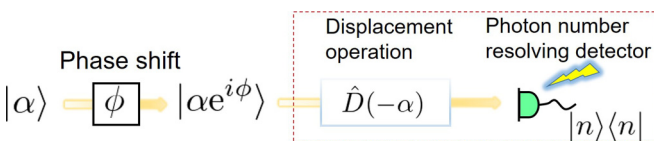


FIG. 2. Schematic of the phase estimation for the coherent state measured by the displaced-photon counting.

experiment it is realized by combining the signal light with a relatively strong local oscillator (LO) light on a beamsplitter with high transmittance. In our scheme, we implement $D(-\alpha)$, which converts the initial probe coherent state $|\alpha\rangle$ to a vacuum. This displacement is followed by a photon-number-resolving detector (PNRD). The measurement operator of the PNRD for n -photon outcome is given by [32]

$$\Pi_n = e^{-\nu} \sum_{l=0}^n \sum_{k=n-l}^{\infty} \frac{\nu^l}{l!} C_{n-l}^k \eta^{n-l} (1-\eta)^{k-(n-l)} |k\rangle\langle k|, \quad (6)$$

where C_{n-l}^k is the binomial coefficient, and ν and η are dark counts and detection efficiency, respectively. For the initial state $|\alpha\rangle$ and a given phase shift ϕ , the conditional probability of detecting n photons is

$$p(n|\phi) = \xi \frac{[2\eta\alpha^2(1-\cos\phi) + \nu]^n}{n!} e^{-2\eta\alpha^2(1-\cos\phi) - \nu} + 2(1-\xi) \frac{(\eta\alpha^2 + \nu)^n}{n!} e^{-\eta\alpha^2 - \nu}. \quad (7)$$

In the ideal case, where $\alpha = \beta$, $\nu = 0$, $\eta = 1$ and the perfect interference visibility ($\xi = 1$) [33], an analytical form of the FI is obtained as

$$F_{\text{dis}}(\phi) = 2\alpha^2(1 + \cos^2\phi). \quad (8)$$

This should be compared with the FIs of the conventional homodyne and heterodyne detections [11,34]. The POVM of the homodyne detection is given by a set of projectors onto quadrature bases $\{\Pi_p = |p\rangle\langle p|\}$ and it implies

$$F_{\text{hom}}(\phi) = 4\alpha^2 \cos^2\phi. \quad (9)$$

The heterodyne detection is composed of a balanced beamsplitter followed by two homodyne detectors for conjugate quadrature components. Its POVM is given by a set of coherent states $\frac{1}{\pi} \{\Pi_\beta = |\beta\rangle\langle\beta|\}$. Though the heterodyne measurement can measure two quadrature amplitudes simultaneously, its performance is limited by the unwanted vacuum fluctuation input from the unused port of the balanced beamsplitter. Thus the QFI is limited to be

$$F_{\text{het}}(\phi) = 2\alpha^2. \quad (10)$$

In Fig. 3 we plot the FIs for the three types of measurements, the displaced-photon counting, the homodyne, and the heterodyne detection. The homodyne detection's FI can reach the QFI at a local point $\phi = 0, \pm\pi$. However, it decreases rapidly as the phase ϕ shifts from this local point, whereas the heterodyne detection's FI is constantly a half of the QFI. We observe that the displaced-photon counting also reaches the QFI at a local phase point $\phi = 0$ and filling the gap between the homodyne and the heterodyne in the sense that it is better than both in a wide region around $\phi = 0$. This might be useful in some applications where the sample's phase is known to be around $\phi = 0$ but has relatively wide fluctuation around there. The FIs of the displaced-photon counting with the imperfections are illustrated in Fig. 4. The performance of the displaced-photon counting is degraded because of the nonunit detection efficiency. Furthermore, in case of the small mean photon number [Fig. 4(a)], the phase-insensitive noises, such as the imperfect visibility and the dark counts, cause

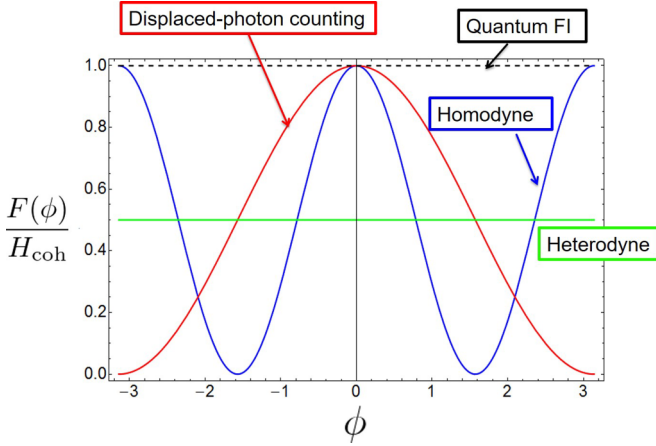


FIG. 3. Fisher information for the displaced-photon counting, the homodyne detection, and the heterodyne detection. The vertical axis is normalized by the quantum Fisher information of the coherent state. Thus the maximum value is 1, where the FI corresponds to the QFI.

high degradation of the FI around $\phi = 0$. This is because the phase-insensitive terms in Eq. (7) become dominant and make the conditional probability less sensitive to the phase shift. In Fig. 4(b), we show the FI of the displaced-photon counting with large coherent amplitude $|\alpha|^2 = 10$. The dark count noise and the imperfect visibility do not make a critical contribution to the conditional probability for the large signal amplitude conditions (see around $\phi = 0$). Thus the scheme is robust against the phase-insensitive noise for larger $|\alpha|^2$ than the weaker probe in Fig. 4(a).

In a real experiment, the measurement outcome from the detector should be postprocessed to estimate the phase value. As a postprocessing algorithm, we choose a standard Bayesian strategy, which is known to saturate the (classical) Cramer-Rao bound $\text{Var}[\hat{\phi}] \geq 1/MF(\phi)$ for large enough M [11].

Suppose $\{n_k\} = \{n_1, n_2, \dots, n_k\}$ is a set of photon numbers observed by the detector after k measurements. Then *a posteriori* probability $P(\phi|\{n_k\})$ of ϕ given $\{n_k\}$ is obtained from a relation

$$p(\{n_k\})P(\phi|\{n_k\}) = p(\phi)P(\{n_k|\phi\}). \quad (11)$$

The prior probability distribution $p(\phi)$ is assumed to be uniform distribution in our estimation and $p(\{n_k\}) = \int_0^\pi p(\phi)P(\{n_k|\phi\})d\phi$ is the prior probability of observing $\{n_k\}$. The latter can be calculated from Eq. (7) and the relation

$$P(\{n_k|\phi\}) = \prod_{i=1}^k p(n_i|\phi). \quad (12)$$

Combining Eqs. (11) and (12) and the uniform $p(\phi)$, we can explicitly derive the form of $P(\phi|\{n_k\})$. Then an expectation value of the estimator and its variance for experimentally measured $\{n_k\}$ are evaluated as

$$\hat{\phi} = \int \phi P(\phi|\{n_k\})d\phi, \quad (13)$$

$$\text{Var}[\hat{\phi}] = \int (\hat{\phi} - \phi)^2 P(\phi|\{n_k\})d\phi. \quad (14)$$

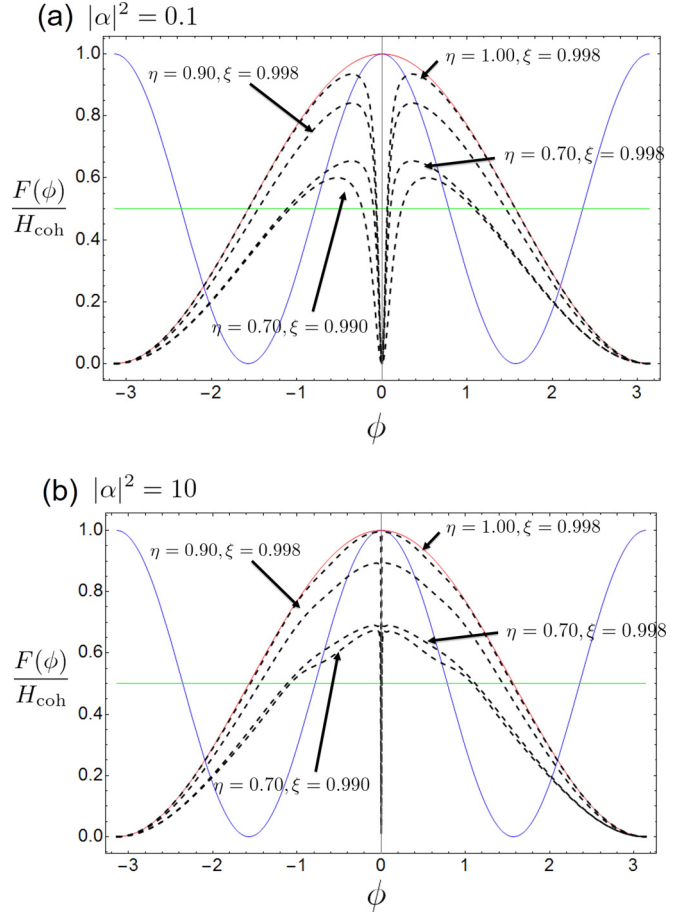


FIG. 4. Normalized FI of the displaced-photon counting with the various imperfect conditions and fixed dark count of 10^{-5} counts per pulse. The mean photon number of the signal state is (a) $|\alpha|^2 = 0.10$ and (b) $|\alpha|^2 = 10$.

III. EXPERIMENT

Figure 5 shows our experimental setup. The continuous-wave laser at 1549 nm is modulated to a sequence of optical pulses with repetition rate of 900 kHz and a pulse width of 100 ns by an acousto-optic modulator (AOM). The optical pulse is sent into a Mach-Zehnder interferometer in which amplitudes of the optical lights are independently controlled by a set including an electro-optic modulator (EOM) and a polarizer. In an optical path for the signal coherent state, a piezotransducer produces the optical phase shift ϕ to be estimated. The signal state with the coherent amplitude α is defined after a fiber coupling and displaced by combining the LO light on an asymmetric fiber coupler with transmittance $\tau = 0.99$. We achieve the visibility $\xi = 0.993$ for the displacement operation. In the experiment, instead of a PNRD, we use a superconducting nanowire single-photon detector (SNSPD), which only discriminates if the photons exist or not [35,36]. The performance gap between the SNSPD and the ideal PNRD are huge when α is large. However, in this proof-of-principle experiment, we choose $\alpha \ll 1$ such that the performance gap between them is in principle negligible because of the extremely small probability of having more than one photon per pulse. We calibrate the optical power of

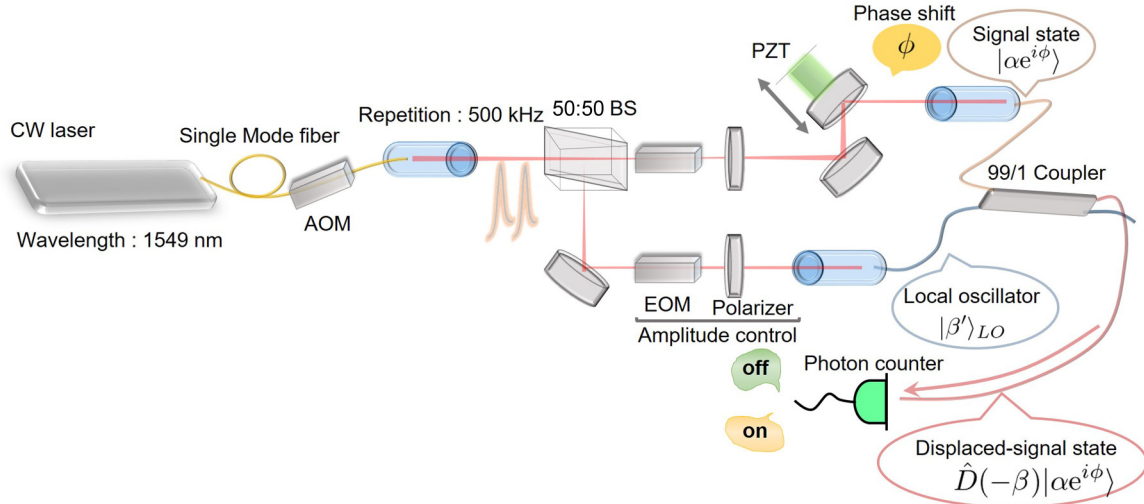


FIG. 5. Experimental setup. AOM: acousto-optic modulator, BS: beamsplitter, EOM: electro-optic modulator, PZT: piezotransducer.

the laser light by using a well-calibrated power meter and then insert a well-calibrated attenuator which reduces the power of the optical light up to single-photon level. The power meter is replaced with the SSPD and, by comparing the expected mean photon number after the attenuation and the detected mean photon number, we obtain the total detection efficiency of our system $\eta = 60.2 \pm 0.4\%$ [37]. Electrical signals from the SNSPD are first transmitted to an SR400 gated photon counter (Stanford Research Systems) which enables us to reduce the dark count to $\nu = 1.13 \times 10^{-4}$ counts/pulse by gating the detection window synchronized with the AOM. The actual phase shift is inferred from 900×10^3 points counted by the SR400 without time information and we simultaneously monitor the electrical signals using an oscilloscope up to 1×10^4 points with time information, which is shown as the experimental results in this paper.

We fix the intensities of the signal state $|\alpha|^2 = 0.100$ and the displacement operation $|\beta|^2 = 0.101$ with the uncertainty 1%. Figure 6 depicts the experimental results for (a) the variance of the estimator and (b) the expectation value when the optical phase shift is set to $\phi \sim 1.00$. In Fig. 6(a), we compare the experimentally evaluated variance of the estimator (gray) with the homodyne detection (blue dashed), the heterodyne detection (green dashed), the displaced-photon counting with (red dashed) and without (red solid) experimental imperfections, and quantum bound derived from the QFI (black dashed). We observe a good agreement between the experimental results and the theoretical predictions. The expectation value estimated from M measurement outcomes is shown by red dots in Fig. 6(b) as a function of the number of measurements M . The black dots in Fig. 6(b) are independently generated by numerical simulation and therefore reflect statistical fluctuation. The expectation value well locates at the actual value of the phase shift (black dashed line) except for the small M . Even though our photon counter and nonunit visibility degrade the performance of the displaced-photon counting, our detection strategy still shows the performance overcoming the homo- and heterodyne detections for the specific phase conditions.

The Bayes theorem guarantees the saturation of the Cramer-Rao inequality for the unbiased estimator if the sample size is infinity. To verify the convergence property for the finite

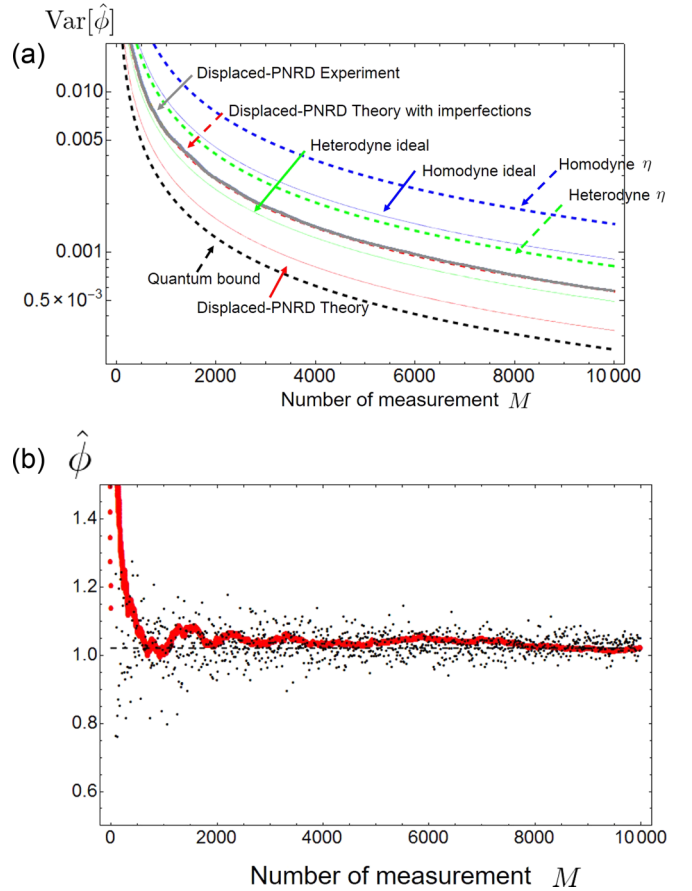


FIG. 6. Experimental results for (a) the variance of the estimator and (b) the expectation value of the estimator (red dot) with the data points generated from numerical simulation (black dot). The phase shift value is fixed to $\phi \sim 1.00$, and the parameters for the experiment are $|\alpha|^2 = 0.100$, $|\beta|^2 = 0.101$, $\xi = 0.993$, $\eta = 60.2\%$, and $\nu = 1.13 \times 10^{-4}$.

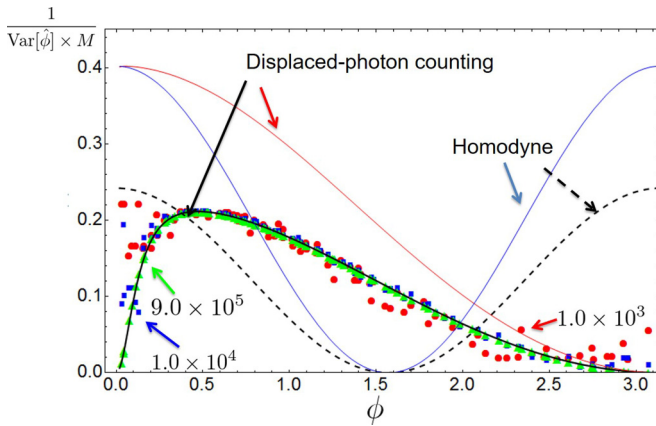


FIG. 7. Inverse of the experimentally obtained variance of the estimator multiplied the number of measurements M . M is set to 1.0×10^3 (red circle), 1.0×10^4 (blue square), and 9.0×10^5 (green triangle). Black solid and dashed lines represent the theoretical FI of the displaced-photon counting and the homodyne detection for the experimental condition $\eta = 0.602$, $\nu = 1.13 \times 10^{-4}$, and $\xi = 0.993$. Red and black solid lines are the theoretical FI of the displaced-photon counting and the homodyne detection in the ideal case.

number of samples, we plot the inverse of the variance multiplied by the number of measurements M in Fig. 7 as a function of the optical phase shift ϕ . The circle (red), square (blue), and triangle (green) plots correspond to the number of measurements $M = 1.0 \times 10^3$, 1.0×10^4 , and 9.0×10^5 , respectively. The ideal FIs without any imperfections for the displaced-photon counting and the homodyne detection are shown by red and blue solid lines, respectively. The experimental data well coincide with the FI of the displaced-photon counting for the experimental condition (solid black line). This coincidence indicates that the Cramer-Rao inequality is saturated with the given number of measurements. However, the discrepancy between the FI and the experimental results becomes apparent when ϕ is extremely small or close to π . The performance overcoming the theoretical FI could occur in the finite samples case because of the statistical randomness of the data acquisition. Note that the variance evaluated from a sufficiently large number of samples or the mean of the variance obtained from independent trials in the same condition satisfies the Cramer-Rao inequality.

IV. CONCLUSION

We proposed and experimentally demonstrated a simple optical phase estimation detector which we call the displaced-photon counting. The detector configuration was inspired by a suboptimal receiver for signal discrimination in quantum optical communication and its application to phase estimation has been examined in both theory and experiment. The theoretical results showed that the displaced-photon counting

exhibits near optimal performance in a wider range of the phase value ϕ than the conventional homodyne detection. The features of the displaced-photon counting offer advantages, especially when the optical phase shift is unknown but supposed to be located around $\phi = 0$. The proof-of-principle of our detection scheme is demonstrated by using the SNSPD as a photon counting device. Though our SNSPD is not ideal (nonunit detection efficiency (60.2%), finite dark counts (1.13×10^{-4} per pulse), and indistinguishability of photon numbers), our results still overcome the ideal limit of homodyne and heterodyne detections around $\phi = 0$. Also, the results well agree with our theoretical predictions, that is, we experimentally observed the saturation of the Cramer-Rao bound via the estimation based on the Bayesian strategy.

There are several interesting future directions. The first possible direction is installation of the PNRD as the photon counter. Though our proof-of-principle experiment with the on/off detector overcomes the homo- and heterodyne limits with a small mean photon number, it does not work for stronger probes, e.g., a few photons per pulse. Moreover, as theoretically show in Sec. II, the PNRD is robust against the phase-insensitive noise by dark counts and the imperfect visibility. The efficiency of the detector is also a critical issue that degrades the performance of our scheme and is required to be almost unity to observe the expected performance. One of the candidates of the desired PNRD satisfying the above conditions is transition edge sensors [37,38]. Another direction is its applications. Our phase estimation strategy using a coherent state provides benefit for an optical metrology, especially because when the signal light is weak, losses are not negligible and sample size is not enough large to utilize an adaptive measurement.

Finally, an interesting future problem is the application of the phase estimation strategy using the displaced-photon counting in optical communication scenarios, such as coherent communication and quantum key distribution (QKD). Although the task in communication is to discriminate the discretely encoded signals with minimum error, the phase estimation is also very important since in practice the receiver has to track the sender's reference frame. In particular, precise monitoring and/or calibrating state preparation is indispensable to ensure the practical implementation security of a QKD system. The phase estimation of the binary encoded coherent states in the binary optical communication is discussed in [39]. Our detailed analysis could be useful for designing a future optical communication system with an extremely weak signal and practical phase tracking.

ACKNOWLEDGMENTS

We acknowledge J. P. Dowling and K. P. Seshadreesan for fruitful discussion. This work was supported by Open Partnership Bilateral Joint Research Projects (JSPS) and the ImpACT Program of Council for Science, Technology and Innovation (Cabinet Office, Government of Japan).

[1] J. P. Dowling and K. P. Seshadreesan, *J. Lightwave Technol.* **33**, 2359 (2015), and references therein.

[2] S. L. Braunstein and C. M. Caves, *Phys. Rev. Lett.* **72**, 3439 (1994).

- [3] A. Monras, *Phys. Rev. A* **73**, 033821 (2006).
- [4] H. Yonezawa, D. Nakane, T. A. Wheatley, K. Iwasawa, S. Takeda, H. Arao, K. Ohki, K. Tsumura, D. W. Berry, T. C. Ralph, H. M. Wiseman, E. H. Huntington, and A. Furusawa, *Science* **337**, 1514 (2012).
- [5] A. A. Berni, T. Gehring, B. M. Nielsen, V. Handchen, M. G. A. Paris, and U. L. Andersen, *Nat. Photonics*, **9**, 577 (2015).
- [6] V. Giovannetti, S. Lloyd, and L. Maccone, *Science* **306**, 1330 (2004).
- [7] T. Nagata, R. Okamoto, J. O'Brien, K. Sasaki, and S. Takeuchi, *Science* **316**, 726 (2007).
- [8] G. Y. Xiang, B. L. Higgins, D. W. Berry, H. M. Wiseman, and G. J. Pryde, *Nat. Photonics* **5**, 43 (2011).
- [9] A. Datta, L. Zhang, N. Thomas-Peter, U. Dorner, B. J. Smith, and I. A. Walmsley, *Phys. Rev. A* **83**, 063836 (2011).
- [10] U. Dorner, R. Demkowicz-Dobrzanski, B. J. Smith, J. S. Lundeen, W. Wasilewski, K. Banaszek, and I. A. Walmsley, *Phys. Rev. Lett.* **102**, 040403 (2009).
- [11] S. Olivares and M. G. A. Paris, *J. Phys. B: At., Mol. Opt. Phys.* **42**, 055506 (2009).
- [12] M. A. Armen, J. K. Au, J. K. Stockton, A. C. Doherty, and H. Mabuchi, *Phys. Rev. Lett.* **89**, 133602 (2002).
- [13] C. W. Helstrom, *Quantum Detection and Estimation Theory* (Academic Press, New York, 1976).
- [14] R. S. Kennedy, Research Laboratory of Electronics, MIT, Quarterly Progress Report No. 108, 1973 (unpublished), p. 219.
- [15] S. Dolinar, Research Laboratory of Electronics, MIT, Quarterly Progress Report No. 111, 1973 (unpublished), p. 115.
- [16] R. S. Bondurant, *Opt. Lett.* **18**, 1896 (1993).
- [17] M. Takeoka, M. Sasaki, and N. Lütkenhaus, *Phys. Rev. Lett.* **97**, 040502 (2006).
- [18] M. Takeoka and M. Sasaki, *Phys. Rev. A* **78**, 022320 (2008).
- [19] S. Guha, J. L. Habif, and M. Takeoka, *J. Mod. Opt.* **58**, 257 (2011).
- [20] S. Izumi, M. Takeoka, M. Fujiwara, N. D. Pozza, A. Assalini, K. Ema, and M. Sasaki, *Phys. Rev. A* **86**, 042328 (2012).
- [21] S. Izumi, M. Takeoka, K. Ema, and M. Sasaki, *Phys. Rev. A* **87**, 042328 (2013).
- [22] R. L. Cook, P. J. Martin, and J. M. Geremia, *Nature (London)* **446**, 774 (2007).
- [23] C. Wittmann, M. Takeoka, K. N. Cassemiro, M. Sasaki, G. Leuchs, and U. L. Andersen, *Phys. Rev. Lett.* **101**, 210501 (2008).
- [24] K. Tsujino, D. Fukuda, G. Fujii, S. Inoue, M. Fujiwara, M. Takeoka, and M. Sasaki, *Opt. Express* **18**, 8107 (2010).
- [25] K. Tsujino, D. Fukuda, G. Fujii, S. Inoue, M. Fujiwara, M. Takeoka, and M. Sasaki, *Phys. Rev. Lett.* **106**, 250503 (2011).
- [26] J. Chen, J. L. Habif, Z. Dutton, R. Lazarus, and S. Guha, *Nat. Photonics* **6**, 374 (2012).
- [27] C. R. Müller, M. A. Usuga, C. Wittmann, M. Takeoka, C. Marquardt, U. L. Andersen, and G. Leuchs, *New J. Phys.* **14**, 083009 (2012).
- [28] F. E. Becerra, J. Fan, G. Baumgartner, J. Goldhar, J. T. Kosloski, and A. Migdall, *Nat. Photonics* **7**, 147 (2013).
- [29] F. E. Becerra, J. Fan, and A. Migdall, *Nat. Photonics* **9**, 48 (2015).
- [30] L. Zhang, H. B. Coldenstrodt-Ronge, A. Datta, G. Puentes, J. S. Lundeen, X. M. Jin, B. J. Smith, M. B. Plenio, and I. A. Walmsley, *Nat. Photonics* **6**, 364 (2012).
- [31] B. Roy Frieden, *Science from Fisher Information* (Cambridge University Press, Cambridge, UK, 2004).
- [32] S. M. Barnett, L. S. Phillips, and D. T. Pegg, *Opt. Commun.* **158**, 45 (1998).
- [33] M. Takeoka, K. Tsujino, and M. Sasaki, *J. Mod. Opt.* **57**, 207 (2010).
- [34] C. Weedbrook, S. Pirandola, R. Garc-Patrn, N. J. Cerf, T. C. Ralph, J. H. Shapiro, and S. Lloyd, *Rev. Mod. Phys.* **84**, 621 (2012).
- [35] S. Miki, T. Yamashita, T. Hirota, and W. Zhen, *Opt. Express* **21**, 10208 (2013).
- [36] T. Yamashita, S. Miki, H. Terai, and Z. Wang, *Opt. Express* **21**, 27177 (2013).
- [37] D. Fukuda, G. Fujii, T. Numata, K. Amemiya, A. Yoshizawa, H. Tsuchida, H. Fujino, H. Ishii, T. Itatani, S. Inoue, and T. Zama, *Opt. Express* **19**, 870 (2011).
- [38] D. Fukuda, G. Fujii, T. Numata, A. Yoshizawa, H. Tsuchida, H. Fujino, H. Ishii, T. Itatani, S. Inoue, and T. Zama, *Metrologia* **46**, S288 (2009).
- [39] M. Bina, A. Allevi, M. Bondani, and S. Olivares, arXiv:1408.0228.